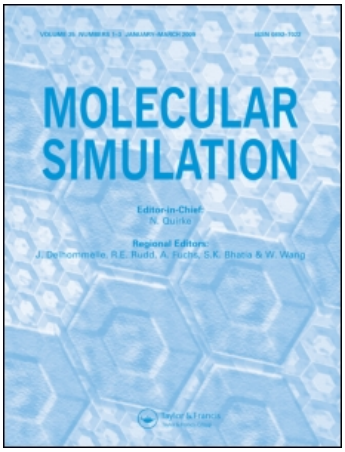

Molecular Simulation
Publication details, including instructions for authors and subscription information:
http://www.informaworld.com/smpp/title~content=t713644482

Prediction of the stability of coiled coils using molecular dynamics simulations

H. Lee[a]; R. G. Larson[b]
[a] Department of Biomedical Engineering, University of Michigan, Ann Arbor, MI, USA [b] Departments of Chemical Engineering, Biomedical Engineering, Mechanical Engineering, and Macromolecular Science and Engineering program, University of Michigan, Ann Arbor, MI, USA

To cite this Article Lee, H. and Larson, R. G.(2007) 'Prediction of the stability of coiled coils using molecular dynamics simulations', Molecular Simulation, 33: 6, 463 — 473
To link to this Article: DOI: 10.1080/08927020701370612
URL: http://dx.doi.org/10.1080/08927020701370612

Molecular Simulation, Vol. 33, No. 6, May 2007, 463–473

Taylor & Francis
Taylor & Francis Group

Prediction of the stability of coiled coils using molecular dynamics simulations

H. LEE† and R. G. LARSON‡*

†Department of Biomedical Engineering, University of Michigan, Ann Arbor, MI 48109, USA
‡Departments of Chemical Engineering, Biomedical Engineering, Mechanical Engineering, and Macromolecular Science and Engineering program, University of Michigan, Ann Arbor, MI 48109, USA

(Received November 2006; in final form March 2007)

We have performed 40–80 ns-long molecular dynamics (MD) simulations of the GCN4 leucine zipper and synthetic coiled coils using the GROMOS96 (43a2) and OPLS-AA force fields, with the aim of predicting coiled coil stability. Starting with an initial configuration of two peptides placed in an ideal coiled coil configuration, we find that changing the amino acid sequence modestly or decreasing peptide length can lead to a decrease in the final α-helicity of coiled coils, although for peptides as long or longer than 16 residues, the values of helicity do not decrease to the low values seen in the experimental results of Lumb *et al.* (*Biochemistry.* **1994**, 33, 7361–7367) or of Su *et al.* (*Biochemistry.* **1994**, 33, 15501–15510), presumably because the simulations are not long enough. We find, however, that helicity correlates positively with the number of close hydrophobic interactions between the two peptides, showing that stable coiled coils in the simulations are tightly packed. The minimum interhelical distances are 0.50–0.66 nm for charged groups, indicating that favorable charge interactions are also important for the stability of the coiled coil.

Keywords: Molecular dynamics simulation; Coiled coil; Peptide stability

1. Introduction

Coiled coils are versatile protein domains, consisting of two or more α-helices wound into a superhelix. Sequences that form coiled coils contain a heptad repeat of seven amino acid residues, which are labeled a–g, with a and d denoting the hydrophobic residues, as shown in figure 1(a) [1,2]. The hydrophobic a and d residues are usually located in the core of the coiled coil, and are thought to play an important role in coiled coil formation. The superhelical structure of coiled coils enables them to assemble into mechanically rigid structures, and thus 2–3% of all protein residues are contained in coiled coils, where they serve as mediators of oligomerization of many proteins such as transcription factors, molecular motors, receptors and signaling molecules [3–5]. Experimental studies of several coiled coils have determined the number of helices they contain, and their orientation, folding and stability [6–10]. These experiments have yielded important information about the effect of specific amino acids in a, d and other positions on the folding and stability of coiled coils. These experimental data have been parameterized and developed into computational programs to predict the existence and structure of coiled coils based on amino acid sequences [11–17]. In particular, the program "SOCKET" was developed to predict the orientation, registry and the number of constituent helices for each detected coiled coil; however this tool can capture only very limited local "knobs-into-holes" packing [16].

While NMR spectrometry, X-ray diffraction, fluorescence resonance energy transfer (FRET), circular dichroism (CD) spectroscopy and other experimental probes provide vital information on the folding and stability of coiled coils, results from these experiments are not always easy to interpret at the atomic level. On the other hand, atomic-level phenomena can be visualized in detail by molecular dynamics (MD) simulations, which offer insights into structure and dynamics, assuming that these simulations can be validated by successful comparisons to available experimental results.

Some MD simulations have already been performed to study the stability of coiled coils. Rozzelle *et al.* [18] simulated the yeast transcriptional activator GCN4 and the designed coiled coils for 300 ps using the GROMOS force

*Corresponding author. Tel.: + 1-734-936-0772. Fax: + 1-734-763-0459. Email: rlarson@umich.edu

Molecular Simulation
ISSN 0892-7022 print/ISSN 1029-0435 online © 2007 Taylor & Francis
http://www.tandf.co.uk/journals
DOI: 10.1080/08927020701370612

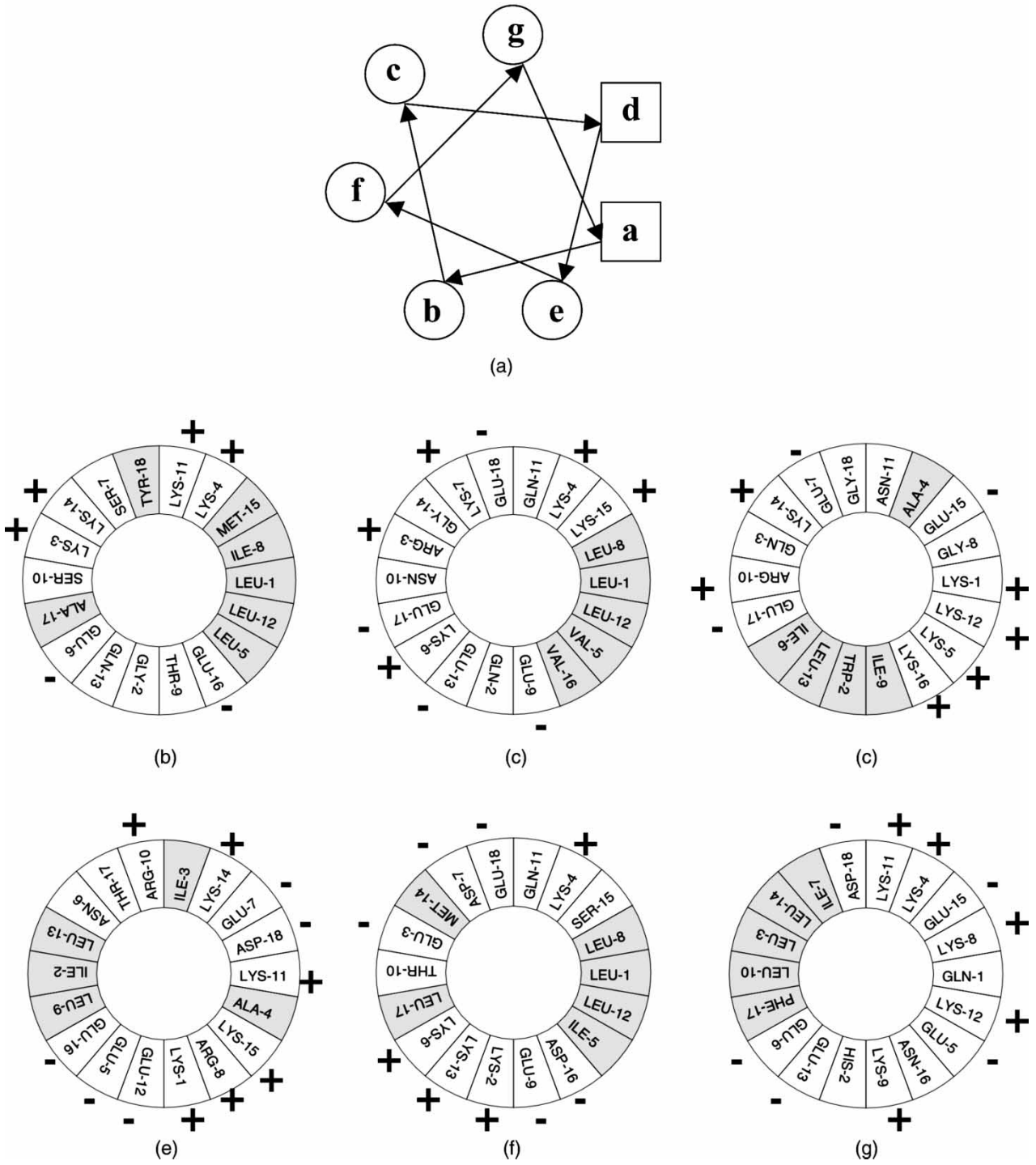

Figure 1. Helical wheel diagrams for (a) the typical coiled coil and for the putative coiled coil domains of (b) KID I, (c) KID II, (d) KID III, (e) KID IV, (f) KID V and (g) KID VI. Amino acid sequences are plotted clockwise. In (a), hydrophobic residues a and d are shown in squares, and the other residues are shown in circles. In (b)–(g), hydrophobic amino acids are shown in gray boxes.

field and showed the effect of interhelical disulfide bonds on the stability of coiled coils. Using the CHARMM 19 force field, Zhong *et al.* [19] simulated a synthetic membrane-spanning ion channel, which consists of a four-stranded coiled coil, for 5 ns, and, using the CVFF force field, Orzechowski *et al.* [20] calculated the binding free energy of some designed coiled coils. Danciulescu *et al.* [21] simulated mutated α-keratin fragments for 200 ps using the GROMOS96 (43a1) force field and calculated their free energies, showing that mutations significantly influence conformational changes of the side chains at the mutation and neighboring sites. Using the GROMOS96 (43a1) force field, Missimer *et al.* [22] simulated a parallel pair of the C-terminal halves and a parallel pair of the N-terminal halves of a twostranded 33-residue leucine zipper of GCN4, and showed that 100 ns-long simulations

cannot distinguish which half is more stable. Recently, the Mark group simulated designed coiled coils over 10 ns using the GROMOS96 (43a2) force field and compared their stability and orientation with experimental results, showing that although the initial structure significantly affects the formation of coiled coils, it was nevertheless possible to predict the preferred orientation of the helices in the coiled coils [23,24]. The Tieleman group has also simulated coiled coils with hydrocarbon interiors over 10 ns using the GROMOS96 (45a3) force field [25].

Although those simulations reveal the possibilities and limitations of MD predictions of the stability and orientation of coiled coils, more comparisons with experiments are necessary to confirm the applicability of MD simulations for structural prediction of coiled coils. Here, we compare simulated with experimentally measured stabilities of shortened versions of the GCN4 leucine zipper [26] and of synthetic coiled coils with different helix lengths [27]. We analyze helical propensity, root mean square deviation (RMSD) between initial and final conformations of backbone atoms of the helices, tightness of the core packing and electrostatic interactions between charged residues. In addition, we use CD spectroscopy to measure the helicity of specially synthesized 18-residue peptides predicted to be coiled coils based on the peptide sequence of a novel protein, Nephrocystin-6 [28], and compare these measurements to simulated structures.

Experimentally, Sayer *et al.* found that mutations in the novel nephronophthisis gene NPHP6/CEP290 cause nephronophthisis type 6, which is the most frequent genetic cause of chronic renal failure in young adults. NPHP6/CEP290 encodes a novel centrosomal protein Nephrocystin-6, with six RepA/Rep$^+$ protein KID domains, which may be involved in chromosome segregation and cell cycle regulation. Those six KID domains are predicted to be a part of coiled coils according to the sequence-based tool COILS2 [12]. Whole coiled coil domains in the protein are too long to simulate using atomistic MD methods, and thus we model only the KID domains as 18 amino acid-long putative amphipathic helices, which are shown in figure 1(b)–(g), and predict possible two-stranded coiled coil structures composed of pairs of these domains using 30–80 ns-long MD simulations. In general, we find that MD simulations are able to correlate coiled coil stability with hydrophobic and charge–charge interactions, but for peptide lengths that are at the border line between stability and instability, the simulations are not yet able reliably to predict *a priori* whether or not a given pair of peptide sequences will form a coiled coil, most likely because the simulations cannot yet be run long enough to fully equilibrate them.

2. Methods

2.1. Computational methods

All simulations and analyses were performed using the GROMACS simulation package [29]. GCN4 leucine zippers were simulated with the GROMOS96 (43a2) force field [30], and synthetic coiled coils were simulated with GROMOS96 (43a2) [30] and OPLS-AA force fields [31]. These force fields were chosen because they have been tested and proven to predict experimentally measured folding structures of the Villin headpiece by van der Spoel and Lindahl [32]. For the shortened versions of GCN4 leucine zipper, we generated 23-amino acid-long α-helices using Swiss-PdbViewer [33], and their sequences are shown in table 1. In the experiments, N- and C-terminal amino groups were respectively acetylated and amidated, making these group neutral. Therefore, in our simulations, the N- and C-termini were respectively unprotonated and protonated to make them electrostatically neutral, to match the terminal charge state of the experimental peptides. Recently, Pineiro *et al.* [24] found that the coiled coil configuration can only be obtained in MD simulations if the initial structure is very close to the expected final configuration. Therefore, two α-helices were aligned in parallel, with the distance between centers of mass of α-helices initially set to 1 nm, which is close to the interhelical distance of typical two-stranded coiled

Table 1. List of simulations for experimentally studied coiled coils, including shortened versions of the GCN4 leucine zipper and parallel coiled coils of synthetic peptides of various lengths. Hydrophobic residues in positions a and d are underlined. Helicities in experiments (Exp. [23,24]) and our simulations (Sim.) are compared. Simulations were performed with GROMOS96 and OPLS-AA force fields. For simulations of GCN4-p1$_{8-30}$ and GCN4-p1$_{11-33}$ using GROMOS96 force field, two values are presented from two simulations with different initial random velocity distributions.

			Helicity (%)		
				Sim.	
	Name	*Sequences*	*Exp.*	*GROMOS96 (40–80 ns)*	*OPLS-AA (50 ns)*
GCN4 leucine zipper	GCN4-p1$_{8-30}$	KVEELLSKNYHLENEVARLKKLV	90	85,85	
	GCN4-p1$_{11-33}$	ELLSKNYHLENEVARLKKLVGER	45	70,76	
Synthetic peptides	SP9	KAEIEACKA	13.7	0	44
	SP12	EALKAEIEACKA	12.1	0	42
	SP16	KAEIEALKAEIEACKA	20.3	72	69
	SP19	EALKAEIEALKAEIEACKA	30.6	71	74
	SP23	KAEIEALKAEIEALKAEIEACKA	74.2	76	78
	SP26	EALKAEIEALKAEIEALKAEIEACKA	89.6	79	83

coils. Approximately, 4900 SPC water molecules were placed around the peptides to a thickness of 1 nm, forming a truncated octahedron. Na^+ and Cl^- ions were added both to neutralize charges from the peptide and to create a concentration of 150 mM NaCl, which is similar to the experimental condition [26]. For the synthetic coiled coils with different lengths and KID domains of NPHP6, the same procedures were performed with different numbers of peptide residues, solvent and ion molecules. SPC water molecules were used for simulations with the GROMOS96 (43a2) force field [30], and TIP4P water molecules were used for simulations with the OPLS-AA force field [31].

A cut-off of 1.4 nm was set for the van der Waals interactions with Particle Mesh Ewald summation used for electrostatic interactions [34]. A pressure of 1 bar and a temperature of 300 K were maintained in an NPT ensemble with a Berendsen pressure coupling and a Berendsen thermostat [35]. The LINCS algorithm was used to constrain the bond lengths [36]. Hydrogen atoms of the peptide were fixed by defining an additional bond of appropriate length between the hydrogen atom and the linked atom, which allows the time step to be increased to 2.5 fs without influencing thermodynamical and dynamical properties of the system. After energy minimization and pre-equilibration with position-restraints, equilibration runs were performed for $40 \sim 80$ ns. The coordinates were saved every picosecond for analysis. Total α-helicity of two peptides in a pair was calculated using the DSSP program [37], averaged over the last 5 ns. The RMSD was calculated between the initial backbone atom coordinates of helices and the coordinates at a later time, and tracked as a function of simulation time. Minimum interhelical distances between charged groups (NH_3^+, $NHCNH_2NH_2^+$ and COO^-, respectively, for Lys, Arg and Glu) of charged residues in positions e and g were also averaged over the last 5 ns. Here, "minimum" distance means the closest distance that can be found between any atom of one charged group and any atom of the other charged group.

2.2 Experimental methods

CD measurements of peptides (100 μM) in buffered solution (10 mM phosphate, pH 7.0) were performed on the aviv model 202 CD spectrometer (Aviv biomedical, lakewood, NJ) with a cell of 0.05 cm path length at 310 K. CD Spectra were obtained by averaging four wavelength scans from 250 to 190 nm at 1 nm intervals. Using the value of $[\theta]_{\text{obs}}$ observed from CD, the ellipticity is reported as the mean residue ellipticity ($[\theta]$, in deg cm^2/dmol) and calculated as

$$[\theta] = [\theta]_{\text{obs}} \left(\frac{\text{MRW}}{10lc} \right),$$

where $[\theta]_{\text{obs}}$ is the ellipticity measured in millidegrees, MRW is the mean residue molecular weight of the polypeptide (molecular weight divided by the number of amino acid residues), c is the concentration of the sample in milligrams/milliliter, and l is the optical path length of the cell in centimeters. Helical formation of the peptide is related to values of ellipticities at 222 nm. Molar ellipticity for a 100% helix ($[\theta]_{222}^{\max}$) of an n-amino acid-long peptide can be calculated as

$$[\theta]_{222}^{\max} = X_H^{\infty} \left(\frac{1-k}{n} \right),$$

where $X_H^{\infty} = -37,400^\circ\,\text{cm}^2$/dmol is the value of $[\theta]_{222}$ for a helix of infinite length, n is the number of residues/helix, and k is a wavelength-dependent constant (2.5 at 222 nm) [38]. Finally, the helicity can be calculated as

$$\text{Percentage peptide helicity} = \frac{[\theta]_{222}}{[\theta]_{222}^{\max}} \times 100$$

3. Results and discussion

We performed 40–80 ns-long MD simulations of coiled coils with known tertiary structure, such as shortened versions of the GCN4 leucine zipper and synthetic coiled coils with different helical lengths. To measure the formation and stability of the coiled coils, we computed the helical propensity, RMSD from perfect helicity for backbone atoms, and tightness of the core packing, and identified the electrostatic interactions between nearby charged residues. We also compared the predicted helicity and close interactions between charged residues with experimental data available from the literature, such as helicity obtained from CD and NMR, and the distances between charged residues obtained from X-ray crystal structure. Although the simulations were performed over a run time of 40–80 ns, the average properties were analyzed only over the last 5 ns when the system was in its most equilibrated state.

3.1. Simulations of shortened versions of the GCN4 leucine zipper

We performed 80 ns-long MD simulations of shortened versions of the GCN4 leucine zipper with explicit water. Here, parallel-oriented pairs of peptides GCN4-$p1_{8-30}$ and GCN4-$p1_{11-33}$ are respectively designated "GCN4-$p1_{8-30}$" and "GCN4-$p1_{11-33}$", as described in table 1. GCN4-$p1_{8-30}$ and GCN4-$p1_{11-33}$, respectively, consist of the 8th–30th and 11th–33rd amino acids out of the 33 amino acids of the full GCN4 leucine zipper, and thus there is a difference of only three residues between GCN4-$p1_{8-30}$ and GCN4-$p1_{11-33}$. Experimentally, Lumb *et al.* [26] found that the helicity of a parallel pair of peptides GCN4-$p1_{8-30}$ is 90%, much higher than that of the parallel pair of peptides GCN4-$p1_{11-33}$, 45%, suggesting that difference of three residues can significantly affect the stability of coiled coils. Figure 2(a),(b) show snapshots

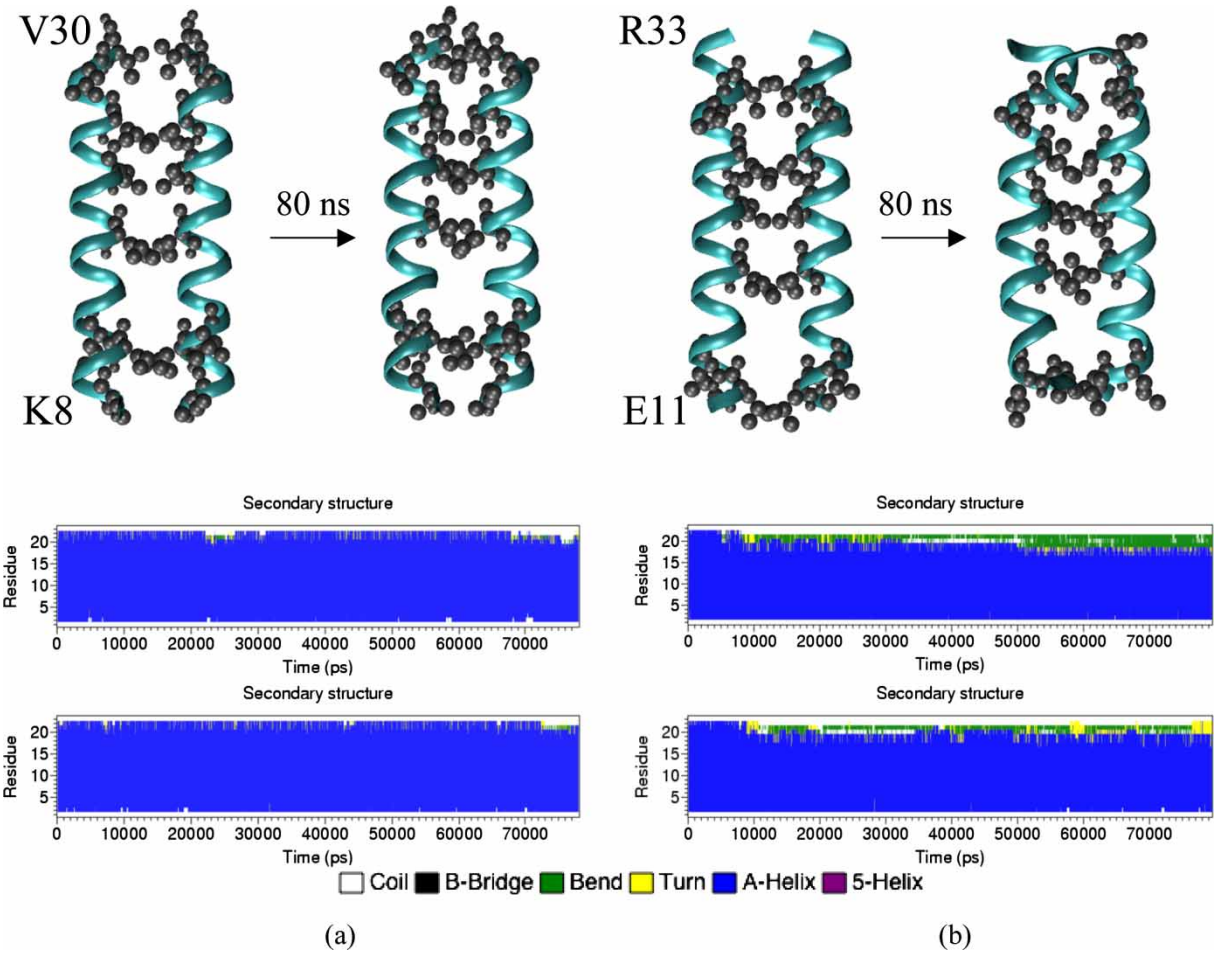

Figure 2. Snapshots at the beginning (0 ns) and end (80 ns) of the simulations (top images) and time dependence of secondary structures (bottom images) of (a) GCN4-p1$_{8-30}$ and (b) GCN4-p1$_{11-33}$. The peptide is represented as a ribbon, and hydrophobic residues in positions a and d are shown as gray dots. The explicit water and ions are omitted for clarity. The images were created using VMD [39]. For both (a) and (b), the top secondary structure profile is for the peptide on the left side of a pair, and the bottom secondary structure profile is for the peptide on the right side of a pair.

from the beginning and end of the simulations (top images) and secondary structure of each peptide (bottom images), respectively, for GCN4-p1$_{8-30}$ and GCN4-p1$_{11-33}$. Although the simulated helical structure of the 29th–33rd residues in GCN4-p1$_{11-33}$ is unstable after 50 ns, with the result that the helicity of GCN4-p1$_{11-33}$ (76%) is less than that of GCN4-p1$_{8-30}$ (85%), the simulations slightly underestimate the helicity for GCN4-p1$_{8-30}$ and greatly overestimate it for GCN4-p1$_{11-33}$, suggesting that the simulations cannot capture significant differences in the stability of peptides with a difference of three residues, at least over timescales of 80 ns. To check the influence of initial velocities, which are generated based on a Maxwell distribution at 300 K, we carried out simulations with the same initial configuration of GCN4-p1$_{8-30}$ and GCN4-p1$_{11-33}$ with different random initial velocities. Table 1 shows that the different initial velocities produce little difference in helicity for either GCN4-p1$_{8-30}$ and GCN4-p1$_{11-33}$, suggesting that different initial velocities do not significantly affect final configurations. In the final structures, stable α-helical structures extending from the 9th to 28th residue and from the 12th to 28th residue were respectively chosen for GCN4-p1$_{8-30}$ and GCN4-p1$_{11-33}$, and their α-helical dimensions (radius, rise/residue and interhelical distance) compare favorably with experimental results obtained by O'Shea *et al.* [40], as shown in table 2. The RMSD between the initial and final backbone atom coordinates of the helices in figure 3(a) is higher for

Table 2. Measurement of α-helical structure. For the simulations, the α-helix radius and rise/residue have two values, one for each of the two peptides in the pair. The error estimates using block averaging are within 0.01 Å.

	Experiment [40]	*Simulation*					
	GCN4-p1	*GCN4-p1$_{8-30}$*	*GCN4-p1$_{11-33}$*	*SP16*	*SP19*	*SP23*	*SP26*
α-helix radius (Å)	2.28	2.33, 2.34	2.31, 2.32	2.26, 2.26	2.32, 2.26	2.31, 2.32	2.31, 2.32
Rise/residue (Å)	1.51	1.50, 1.50	1.50, 1.50	1.53, 1.54	1.49, 1.54	1.51, 1.50	1.52, 1.51
Interhelical distance (Å)	9.8	9.8	9.8	8.8	10.0	10.1	9.7

GCN4-p1$_{11-33}$ than for GCN4-p1$_{8-30}$, suggesting that GCN4-p1$_{8-30}$ is the more stable, which is consistent with the relative helical stability of these coiled coils.

In addition to the helical propensity, the tightness of the core packing and presence of favorable interactions between charged residues are also important measures of the stability of coiled coils [1]. To analyze the tightness of core packing, the number of close interhelical interactions between hydrophobic residues in positions a and d on different peptides was calculated every timestep and averaged over the last 5 ns, as shown in table 3. If the interhelical distance between each C_β atom of these hydrophobic residues on different peptides is within 0.6 nm, the interaction is considered to be "close." Table 3 reports that there are around eight close interhelical interactions between hydrophobic residues for each of the coiled coils formed by GCN4-p1$_{8-30}$ and GCN4-p1$_{11-33}$, showing that those hydrophobic cores are tightly packed. To understand the effect of different numbers of hydrophobic residues in positions a and d on the helical stability, synthetic peptides with different lengths were simulated, which will be discussed in the next section.

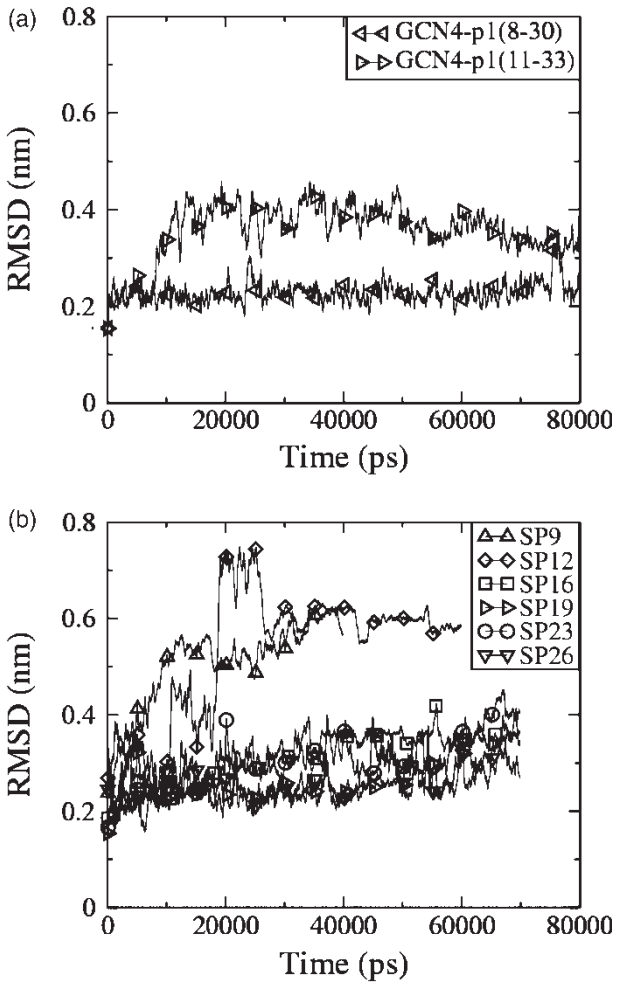

Figure 3. RMSD between starting atomic coordinates and coordinates at time t averaged over backbone atoms of helices for (a) GCN4-p1$_{8-30}$ and GCN4-p1$_{11-33}$ and (b) synthetic peptides with different lengths. Data were averaged over 50 ps intervals.

Table 3. The number of close interhelical interactions ($\leq$0.6 nm) between C_β atoms of hydrophobic residues in positions a and d on different peptides, averaged over the last 5 ns.

	Number of close interhelical interactions ($\leq$0.6 nm) between C_β atoms of hydrophobic residues
GCN4-p1$_{8-30}$	7.91 ± 0.72
GCN4-p1$_{11-33}$	7.96 ± 0.14
SP9	0.71 ± 0.11
SP12	0
SP16	2.25 ± 0.08
SP19	3.36 ± 0.08
SP23	3.66 ± 0.18
SP26	5.17 ± 0.20

Although the roles of residues in positions e and g are less understood than those in positions a and d, experiments and simulations have revealed the importance for the stability of the coiled coil of the charge interactions between residues in positions e or g on one peptide and e or g on the other [1,2]. Since residues in the hydrophobic core (positions a and d) of the two peptides in a pair face each other, when the two peptides form a parallel two-stranded coiled coil, the residues in positions e and g of one peptide can respectively interact with a residue in either positions g′ or e′ of the other (these interactions are termed, respectively, "e–g′" and "g–e′" interactions, where the prime denotes the positions on the second peptide). Both GCN4-p1$_{8-30}$ and GCN4-p1$_{11-33}$ form parallel two-stranded coiled coils, and thus e–g′ and/or g–e′ are the allowed interhelical interactions between charged residues. To analyze favorable electrostatic interactions, the smallest interhelical distances between any atom of the charged groups (NH_3^+, $NHCNH_2NH_2^+$ and COO^-, respectively, for Lys, Arg and Glu) of charged residues at positions e on one peptide and g′ on the other were measured every picosecond and averaged over the last 5 ns, and likewise for the charged groups at positions g and e′, and are shown in table 4. Because the two peptides in the coiled coil are identical in this case, interactions e–g′ and e′–g are identical. Therefore, values of e–g′ and e′–g distances are almost the same, and can be either rather small, around 0.50–0.66 nm (bold text) or rather large, 0.93–2.30 nm, as shown in table 4. For GCN4-p1$_{8-30}$, small distances of 0.52–0.66 nm are measured between K15 (or E20) on one peptide and E20 (or K15) on the other for g–e′ (or g′–e), and between E22 (or K27) on one peptide and K27 (or E22) on the other for g–e′ (or g′–e), indicating that interactions between Lys and Glu are attractive, as shown in figure 4. These distances correspond closely to the experimental results measured by O'Shea *et al.* [40], who showed using X-ray crystal structure that interhelical ion pairs in 33-amino acid-long GCN4-p1$_{1-33}$ are formed between K15 and E20, and E22 and K27.

One might expect that K15 in position g and E20 in position e′ on different peptides in GCN4-p1$_{11-33}$ might attract each other, as was observed in GCN4-p1$_{8-30}$. However, for GCN4-p1$_{11-33}$ their separation is not at all

Table 4. The closest interhelical distances (in nm) between charged groups (NH_3^+, $NHCNH_2NH_2^+$ and COO^-, respectively, for Lys, Arg, Glu and Asp) of each charged residue in positions e and g on different peptides, averaged over the last 5 ns of the simulations. Pairs with distances of ≤0.66 nm are in bold type. The numbers following the initial representing the amino acid (e.g. "20" in "K20") stands for the residue number.

GCN4-p1$_{8-30}$ (helicity: 85%)	e–g′	Pairs	E20(−)–K8(+)	**E20(−)–K15(+)**	E20(−)–E22(−)	K27(+)–K8(+)	K27(+)–E22(−)
		Distance	1.45 ± 0.05	**0.66 ± 0.04**	1.03 ± 0.01	2.30 ± 0.04	**0.52 ± 0.02**
	e′–g	Pairs	E20(−)–K8(+)	**E20(−)–K15(+)**	E20(−)–E22(−)	K27(+)–K8(+)	K27(+)–E22(−)
		Distance	1.41 ± 0.06	**0.66 ± 0.05**	1.04 ± 0.01	2.18 ± 0.06	**0.55 ± 0.02**
GCN4-p11–33 (Helicity: 76%)	e–g′	Pairs	E20(−)–K15(+)	K27(+)–K15(+)	E20(−)–E22(−)	**K27(+)–E22(−)**	
		Distance	1.01 ± 0.01	1.54 ± 0.03	1.03 ± 0.02	**0.50 ± 0.03**	
	e′–g	Pairs	E20(−)K15(+)	K27(+)–K15(+)	E20(−)–E22(−)	**K27(+)–E22(−)**	
		Distance	0.93 ± 0.02	1.53 ± 0.03	1.03 ± 0.01	**0.54 ± 0.02**	

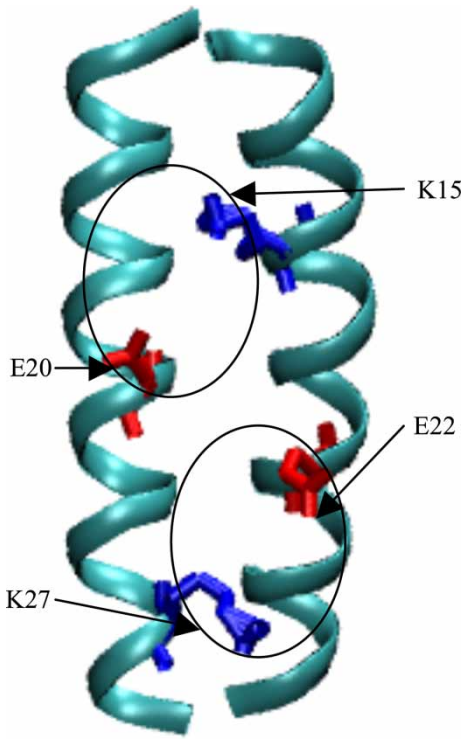

Figure 4. Attractive interhelical interactions between lysine (blue) and glutamic acid (red) residues in GCN4-p1$_{8-30}$. The two e–g′ interactions are shown, and the g–e′ interactions are omitted for clarity (colour online).

small (0.93–1.01 nm), showing no attractive interhelical interactions between them. From the X-ray structure, O'Shea *et al.* [40] showed that for GCN4-p1$_{1-33}$, there is a close intrahelical contact between the lysine residue K8 in position g and the spatially proximate E11 in position c on the same peptide (3.3 Å), suggesting that this intrahelical interaction between K8 and E11 leaves K15 in position g free to interact interhelically with E20 in position e′. From our simulations, in GCN4-p1$_{8-30}$ containing K8, the expected close interhelical interaction between K15 and E20 is observed, similar to experimental results, whereas, in GCN4-p1$_{11-33}$, this lysine K8 is missing, and so E11 interacts intrahelically with K15, making it unavailable to form an ion pair interhelically with E20. This seems to explain the large interhelical separation between K15 and E20, confirming the experimentally-suggested role of K8. This suggests that the competition between inter- and intrahelical ion pairs affects coiled coil structure [40]. These results indicate that MD simulations might be able to capture experimentally relevant factors controlling the stability of coiled coils, such as electrostatic interactions, even when the predictions of overall helicity are not very accurate.

3.2. Simulations of synthetic coiled coils with different lengths

We performed 70 ns-long simulations of synthetic coiled coils of different lengths in explicit water to understand

the effect of different numbers of hydrophobic residues in positions a and d on the helical stability. Parallel pairs of synthetic coiled coils named "SP9", "SP12", "SP16", "SP19", "SP23" and "SP26", which respectively contain 9, 12, 16, 19, 23 and 26 amino acids with the same repeats of the sequence IEALKAE, are described in table 1. Experimentally, Su *et al.* [27] designed these synthetic peptides to determine the minimum chain length required to stabilize an α-helical coiled coil. By measuring the α-helical structure and ellipticity ratio from CD spectroscopy they showed that a minimum of three heptads is required for a peptide to adopt the two-stranded α-helical coiled coil in aqueous solution [27]. Figure 5 shows simulated secondary structures of each peptide for SP9–SP26. Our simulations show that α-helical structures of SP9 and SP12 are completely broken within 3 ns. On the other hand, SP16 and SP19 have a stable α-helical structure with unfolding coils or turns in some regions, and SP23 and SP26 have relatively stable α-helical structures. In table 1, for simulations with the GROMOS96 force field, peptide helicities from the simulations are in agreement with experimental values from CD spectroscopy by Su *et al.* [27] for SP9 and SP12 as well as SP23 and SP26. However, for SP16 and SP19, the helicities in the simulations are much higher than in the experiments presumably because for the cases of marginal stability 70 ns is not long enough to observe protein unfolding. For simulations with the OPLS-AA force field,

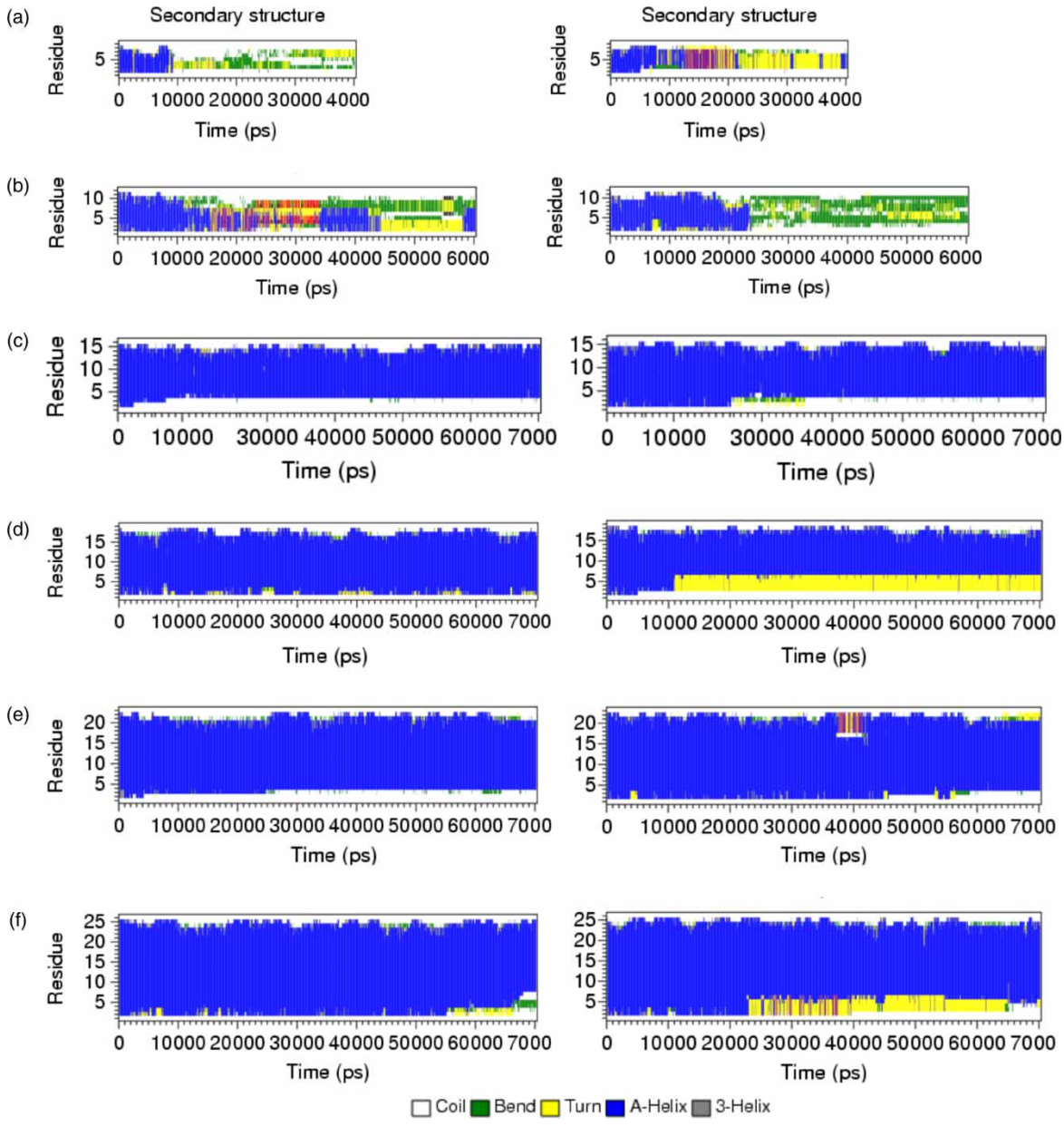

Figure 5. Secondary structure profiles of each peptide in parallel-oriented dimers of (a) SP9, (b) SP12, (c) SP16, (d) SP19, (e) SP23 and (f) SP26 as a function of time.

similar over-predictions are observed for SP16, SP19, SP23 and SP26, and in addition, the helicities of SP9 and SP12 are also overestimated. Although a difference between the helicities of SP12 and SP16 is observed in the simulations using GROMOS96, the difference is not found when using OPLS-AA, suggesting that GROMOS96 represents the instability of these coiled coil peptides better than does OPLS-AA, although the two different force fields show similar over-predictions of helicity for shorter peptides. These results suggest that the failure to predict helicity correctly is likely due to an inadequate period of equilibration, rather than with the force field, although the possibility of problems with both force fields cannot be ruled out. Note that while the 23-residue peptide was stable for this peptide sequence, the 23-residue peptide GCN4-p1$_{11-33}$ was experimentally unstable, but that, as discussed above, this instability was not correctly captured by the 80-ns simulations. Thus, simulations of this duration are evidently not able to capture the instability of coiled coils made of peptides with 16 or more residues.

Nevertheless, the α-helical parameters (radius, rise/residue and interhelical distance) from the simulations are similar to the experimentally measured values, as shown in table 2. Figure 3(b) shows that RMSD's between the final and initial backbone atoms of SP9 and SP12 are higher than those for SP16, SP19, SP23 and SP26, showing again that helices of SP9 and SP12 are more unstable than the others, which is consistent with the observed helicity. Table 3 shows that SP23 and SP26 have more interhelical hydrophobic interactions than do the others, showing that peptides with longer length are more tightly packed due to their interhelical hydrophobic interactions.

3.3 Stability of pairs of six KID domains using MD simulations and CD spectroscopy

As described above, our 80-ns MD simulations correctly predict the stability of coiled coils of length 23 residues or more, and the instability of those of length 12 or less, but do not correctly predict the observed instability of two-stranded coiled coils with 16 or more amino acids. To see if this inability to predict the instability of intermediate-length coiled coils is a general feature of our simulation methods, we now describe 30–80 ns-long MD simulations of pairs of six 18-residue KID domains, which are parts of a newly discovered protein, NPHP6 [28]. Considering all possible pairs of 6 domains, including self-pairs, each in a parallel and an antiparallel orientation, there are 42 different possible coiled coil pairs. Those 42 pairs were simulated starting from the optimal coiled coil configuration. Since it has been experimentally observed that at least 21–23 amino acids are required for the formation of two-stranded coiled coils [26,27,41,42], helices of all 42 pairs are expected to be unfolded. However, the simulations show a broad range of final helicities, 22–86%, after 80 ns of simulation, including three pairs

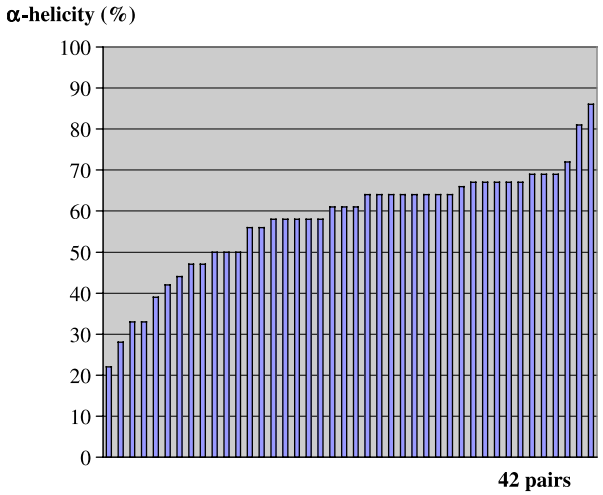

Figure 6. Distribution of α-helicity of 42 different pairs of KID domains at the end of the 80-ns simulations.

that have high helicity of 72–86%, as shown in figure 6. To confirm our expectation that these peptides are too short to form stable coiled coils, we experimentally measured the helicity of one of the pairs predicted by the simulations of KID III/KID VI to have the highest helicity (81%) using CD spectroscopy. We found, as expected, that the experimentally determined helicity of this pair is only 22%, which is much lower than that observed from the simulation. This experimental result confirms that 80-ns simulations using the GROMOS96, or perhaps any force field, cannot be relied on to predict accurately the helical propensities of possible coiled coil-forming peptides, at least for peptides with 16 or more residues.

4. Conclusions

We performed 40–80 ns-long MD simulations of experimentally studied coiled coils including the GCN4 leucine zipper and synthetic coiled coils with different helical lengths to compare the predicted to experimentally measured coiled coil stability. The 40–80 ns simulations using the GROMOS96 (43a2) and OPLS-AA force fields show a trend of decreasing stability with decreasing peptide length similar to that for the experimentally measured α-helicity, but the instability of coiled coils of length 16 or more residues is not captured by the simulations with either force field. This shows that simulations cannot yet reliably predict the differences in stability of peptides with different residues or with different helical lengths, presumably at least in part because of the limitation of simulation timescale. RMSD's for backbone atoms between initial and final conformations show that peptides with higher α-helicity remain closer to the initial structure, confirming that peptides with higher α-helicity are more stable. More interhelical interactions between hydrophobic residues in positions a and d on different peptides are observed in the peptides

with higher helicity, and minimum interhelical distances of 0.50–0.66 nm between charged groups of charged residues in positions e and g are also observed in stable coiled coils, confirming that favorable hydrophobic and charge interactions are important for the stability of coiled coils. These results suggest that MD simulations can predict favorable electrostatic interactions of coiled coils, but cannot yet accurately predict helical propensity, except for peptides shorter than 16 residues, unless timescales much longer than 80 ns are accessed.

Acknowledgements

We gratefully acknowledge the help of Friedhelm Hildebrandt in the Departments of Pediatrics and of Human Genetics, A. Ramamoorthy in the Department of Chemistry, and Senthil Kandasamy, a member of our research group, for valuable discussions.

References

[1] A.N. Lupas, M. Gruber. The structure of α-helical coiled coils. *Adv. Protein Chem.*, **70**, 37 (2005).
[2] D.N. Woolfson. The design of coiled-coil structures and assemblies. *Adv. Protein Chem.*, **70**, 79 (2005).
[3] M. Gruber, A.N. Lupas. Historical review: another 50th anniversary—new periodicities in coiled coils. *Trends Biochem. Sci.*, **21**, 375 (2003).
[4] P. Burkhard, J. Stetefeld, S.V. Strelkov. Coiled coils: a highly versatile protein folding motif. *Trends Cell Biol.*, **11**, 82 (2001).
[5] A. Rose, I. Meier. Scaffolds, levers, rods and springs: diverse cellular functions of long coiled-coil proteins. *Cell. Mol. Life Sci.*, **61**, 1996 (2004).
[6] O.D. Monera, C.M. Kay, R.S. Hodges. Electrostatic interactions control the parallel and antiparallel orientation of α-helical chains in two-stranded α-helical coiled-coils. *Biochemistry*, **33**, 3862 (1994).
[7] J.A. Zitzewitz, B. Ibarra-Molero, D.R. Fishel, K.L. Terry, C.R. Matthews. Preformed secondary structure drives the association reaction of GCN4-p1, a model coiled-coil system. *J. Mol. Biol.*, **296**, 1105 (2000).
[8] J.A. Knappenberger, J.E. Smith, S.H. Thorpe, J.A. Zitzewitz, C.R. Matthews. A buried polar residue in the hydrophobic interface of the coiled-coil peptide, GCN4-p1, plays a thermodynamics, not a kinetic role in folding. *J. Mol. Biol.*, **321**, 1 (2002).
[9] B. Ibarra-Molero, J.A. Zitzewitz, C.R. Matthews. Salt-bridges can stabilize but do not accelerate the folding of the homodimeric coiled-coil peptide GCN4-p1. *J. Mol. Biol.*, **336**, 989 (2004).
[10] J.R. Litowski, R.S. Hodges. Designing heterodimeric two-stranded α-helical coiled-coils: the effect of chain length on protein folding, stability and specificity. *J. Pept. Res.*, **58**, 477 (2001).
[11] A. Lupas. Predicting coiled coils regions in proteins. *Curr. Opin. Struct. Biol.*, **7**, 388 (1997).
[12] A. Lupas, M. van Dyke, J. Stock. Predicting coiled coils from protein sequences. *Science*, **252**, 1162 (1991).
[13] B. Berger, D.B. Wilson, E. Wolf, T. Tonchev, M. Milla, P.S. Kim. Predicting coiled coils by use of pairwise residue correlations. *Proc. Natl. Acad. Sci. USA*, **92**, 8259 (1995).
[14] D.N. Woolfson, T. Alber. Predicting oligomerization states of coiled coils. *Protein Sci.*, **4**, 1596 (1995).
[15] E. Wolf, P.S. Kim, B. Berger. Multicoil: a program for predicting two- and three stranded coiled coils. *Protein Sci.*, **6**, 1179 (1997).
[16] J. Walshaw, D.N. Woolfson. SOCKET: a program for identifying and analyzing coiled coil motifs within protein structures. *J. Mol. Biol.*, **307**, 1427 (2001).
[17] M. Gruber, J. Soding, A.N. Lupas. REPPER-repeats and their periodicities in fibrous proteins. *Nucleic Acids Res.*, **33**, 239 (2005).
[18] J.E. Rozzelle Jr., A. Tropsha, B.W. Erickson. Rational design of a three-heptad coiled-coil protein and comparison by molecular dynamics simulation with the GCN4 coiled coil: presence of interior three-center hydrogen bonds. *Protein Sci.*, **3**, 345 (1994).
[19] Q. Zhong, Q. Jiang, P.B. Moore, D.M. Newns, M.L. Klein. Molecular dynamics simulation of a synthetic ion channel. *Biophys. J.*, **74**, 3 (1998).
[20] M. Orzechowski, P. Cieplak, L. Piela. Theoretical calculation of the coiled-coil stability in water in the context of its possible use as a molecular rack. *J. Comput. Chem.*, **23**, 106 (2002).
[21] C. Danciulescu, B. Nick, F. Wortmann. Structural stability of wild type and mutated α-keratin fragments: molecular dynamics and free energy calculations. *Biomacromolecules*, **5**, 2165 (2004).
[22] J.H. Missimer, M.O. Steinmetz, W. Jahnke, F.K. Winkler, W.F. van Gunsteren, X. Daura. Molecular-dynamics simulations of C- and N-terminal peptide derivatives of GCN4-p1 in aqueous solution. *Chem. Biodiversity*, **2**, 1086 (2005).
[23] K. Pagel, K. Seeger, B. Seiwert, A. Villa, A.E. Mark, S. Berger, B. Koksch. Advanced approaches for the characterization of a de novo designed antiparallel coiled coil peptide. *Org. Biomol. Chem.*, **3**, 1189 (2005).
[24] A. Pineiro, A. Villa, T. Vagt, B. Koksch, A.E. Mark. A molecular dynamics study of the formation, stability, and oligomerization state of two designed coiled coils: possibilities and limitations. *Biophys. J.*, **89**, 3701 (2005).
[25] E. Kelly, G.G. Prive, D.P. Tieleman. Molecular models of lipopeptide detergents: large coiled-coils with hydrocarbon interiors. *J. Am. Chem. Soc.*, **127**, 13446 (2005).
[26] K.J. Lumb, C.M. Carr, P.S. Kim. Subdomain folding of the coiled coil leucine zipper from the bZIP transcriptional activator GCN4. *Biochemistry*, **33**, 7361 (1994).
[27] J.Y. Su, R.S. Hodges, C.M. Kay. Effect of chain length on the formation and stability of synthetic α-helical coiled coils. *Biochemistry*, **33**, 15501 (1994).
[28] J.A. Sayer, E.A. Otto, J.F. O'Toole, G. Nurnberg, M.A. Kennedy, C. Becker, H.C. Hennies, J. Helou, M. Attanasio, B. Fausett, B. Utsch, H. Khanna, Y. Liu, L. Drummond, I. Kawakami, T. Kusakabe, M. Tsuda, L. Ma, H. Lee, R.G. Larson, S.J. Allen, C.J. Wilkinson, E.A. Nigg, C. Shou, C. Lillo, D. Williams, B. Hoppe, M. Kemper, T. Neuhaus, M. Petry, A. Kispert, Y. Zou, J. Gloy, A. Ganner, G. Walz, X. Zhu, D. Goldman, P. Nurnberg, A. Swaroop, M.R. Leroux, F. Hildebrandt. The centrosomal protein nephrocystin-6 is mutated in joubert syndrome and activates transcription factor ATF4. *Nat. Genet.*, **38**, 674 (2006).
[29] E. Lindahl, B. Hess, D. van der Spoel. GROMACS 3.0: a package for molecular simulation and trajectory analysis. *J. Mol. Mod.*, **7**, 306 (2001).
[30] W.F. van Gunsteren, S.R. Billeter, A.A. Eising, P.H. Hunenberger, P. Kruger, A.E. Mark, W.R.P. Scott, I. Tironi. *Biomolecular Simulation: The GROMOS96 Manual and User Guide*, Zurich, Switzerland (1996).
[31] W.L. Jorgensen, J. Tirado-Rives. The OPLS potential functions for proteins. Energy minimization for crystals of cyclic peptides and crambin. *J. Am. Chem. Soc.*, **110**, 1657 (1988).
[32] D. van der Spoel, E. Lindahl. Brute-force molecular dynamics simulations of villin headpiece: comparison with NMR parameters. *J. Phys. Chem. B*, **107**, 11178 (2003).
[33] N. Guex, M.C. Peitsch. SWISS-MODEL and the Swiss-PdbViewer: an environment for comparative protein modeling. *Electrophoresis*, **18**, 2714 (1997).
[34] U. Essmann, L. Perera, M.L. Berkowitz, T. Darden, H. Lee, L.G. Pedersen. A smooth particle mesh Ewald method. *J. Chem. Phys.*, **103**, 8577 (1995).
[35] H.J.C. Berendsen, J.P.M. Postma, W.F. van Gunsteren, A. Dinola, J.R. Haak. Molecular dynamics with coupling to an external bath. *J. Chem. Phys.*, **81**, 3684 (1984).
[36] B. Hess, H. Bekker, H.J.C. Berendsen, J.G.E.M. Fraaije. LINCS: a linear constraint solver for molecular simulations. *J. Comp. Chem.*, **18**, 1463 (1997).
[37] W. Kabsch, C. Sander. Dictionary of protein secondary structure: pattern recognition of hydrogen-bonded and geometrical features. *Biopolymers*, **22**, 2577 (1983).

[38] Y.H. Chen, J.T. Yang, K.H. Chau. Determination of the helix and beta form of proteins in aqueous solution by circular dichroism. *Biochemistry*, **13**, 3350 (1974).
[39] W. Humphrey, A. Dalke, K. Schulten. VMD—visual molecular dynamics. *J. Mol. Graph.*, **14**, 33 (1996).
[40] E.K. O'Shea, J.D. Klemm, P.S. Kim, T. Alber. X-ray structure of the GCN4 leucine zipper, a two-stranded, parallel coiled coil. *Science*, **254**, 539 (1991).
[41] R. Fairman, H.G. Chao, L. Mueller, T.B. Lavoie, L. Shen, Y. Novotny, G.R. Matsueda. Characterization of a new four-chain coiled-coil: influence of chain length on stability. *Protein Sci.*, **4**, 1457 (1995).
[42] R.A. Kammerer, T. Schulthess, R. Landwehr, A. Lustig, J. Engel, U. Aebi, M.O. Steinmetz. An autonomous folding unit mediates the assembly of two-stranded coiled coils. *Proc. Natl. Acad. Sci. USA*, **95**, 13419 (1998).